[1]Ibrahim Ramadhan Agool

[2]Ali Taher Mohi

[3]Mahir Noori Thameel

[4]Yasmeen Z. Dawood

[5]Nadir Fadhil Habubi

[6]Sami Salman Chiad

# Physical Characterization of Antimony Doped Nanostructured Nickel Oxide Thin Films

***Abstract: -*** Antimony Doped NiO and nanostructured NiO films were produced using Simple Spray Pyrolysis (SP). The anticipated films were polycrystalline, with a favored peak along the (200) plane, according to an XRD examination. The grain size had decreased from a maximum of 17.81 nm to 28.49 nm at 3% antimony doping. Calculations were made for micro strain and dislocation density, among other microstructural characteristics. Findings came in. The morphology of the surface (AFM) of the film is affected by this antimony. The (Undoes) nanoparticles' average particle sizes were discovered to be 87.5, 49.7, and 41.6 nm. NiO: (Ra) and (Rrms) of AFM: NiO, undated NiO, NiO with 1% Sb, and NiO with 3% Sb, respectively Sb films have a wavelength range of (10.71-5.26) nm and (8.76 - 3.32 nm). Using UV-visible transmission spectroscopy, it was discovered that the deposited films are transparent in the visible spectrum. The refractive index and extinction coefficient both decrease with antimony concentration and the energy gap was 3.63–3.52 eV.

***Keywords:*** NiO, Sb, thin films, XRD, Morphology, Optical Properties, band gap

## I. Introduction

NiO is a p-type film because of its excellent properties, which include great chemical stability, strong crystal clear, a direct energy gap of 3.6–4.0 eV, a high transparency spectrum, and a low material cost [4]. By increasing the quantity of interstitial oxygen and/or Ni vacancies when NiO is present, the resistivity of undated NiO films is dramatically decreased [5,6]. The stoichiometric balance between the nickel and oxygen atoms has a big impact on the behavior of NiO. They go through a variety of modifications as a result of their nonstoichiometric, which have a variety of effects on a variety of applications, including organic light-emitting diodes [11], electrodes in solar cells [8, 9], gas sensors [10], and electro chromic materials [7]. There are several different types of nickel oxide, including NiO, $NiO_2$, $NiO_4$, and $Ni_2O_3$. Bulk NiO has a high melting point (2000 °C) and a very high resistivity, indicating that high-temperature applications are possible for it. Because $Ni^{2+}$ vacancies are created in the NiO structure when heated in air, NiO exhibits p-type semi conductivity [12]. NiO films were produced using a comprehensive various techniques, such as reactive sputtering [13], PECVD [5], EBE [6], sol-gel [14] and SP [15-17]. Compared to the other technique, the spray pyrolysis method is much simpler, less expensive, safer, and less expensive overall as a non-vacuum system of deposition method [4]. This method is used to manufacture transparent conducting oxides. Spray pyrolysis has several benefits over

[1] Bilad Alrafidain University College, *Diyala, Iraq*
dr.agool@bauc14.edu.iq
[2]*Dept. Physics College of Education, Mustansiriyah University Baghdad, Iraq*
dr.alitaher@uomustansiriyah.edu.iq
[3]*Dept. Physics College of Education for Pure science, University of Anbar Anbar, Iraq*
esp.mahern.thumail@uoanbar.edu.iq
[4]*Dept. Physics College of Education, Mustansiriyah University Baghdad, Iraq*
yasmeen.zaidan@uomustansiriyah.edu.iq
[5]*Dept. Engineering of Refrigeration and Air Conditioning Technologies Alnukhba University College Baghdad, Iraq*
n.fadhil@alnukhba.edu.iq
[6]*Dept. Physics College of Education, Mustansiriyah University Baghdad, Iraq*
dr.sami@uomustansiriyah.edu.iq

traditional pneumatic spraying, the most notable of which are its reduced material consumption, improved capacity to regulate moderate carrier gas circulation and splash, all of which make it possible to deposit very thin layers of a steady thickness [18]. In this paper, we stared into how antimony affected the characterization of NiO thin films, which is essential for a more profound comprehension and improvement of the material quality.

## II. EXPERIMENTAL

A spray pyrolysis coating unit was incorporated inside the device to deposit NiO and NiO: Sb thin films. The right proportions of nickel chloride ($NiCl_3$) (0.1M) dissolved in deionized water were combined to create the spray solution. Antimony dichloride ($SbCl_3$) was resolved in a solution of is then incorporated into the combination to accomplish Sb doping. The doping concentration of (0, 1, 3%). The conditions for preparation: In order to prevent cooling, the spraying period of 10 seconds was extended by 100 seconds. The base temperature was 400°C, and the vehicle gas used was nitrogen. A measuring method was implemented to determine the the movie's dimension, which came out as being 340±25 nm. Using a UV-visible shiatsu double beam spectrophotometer, optical transmittance spectra for as-deposited thin films were evaluated. The nature of film structure was ascertained using XRD, and film surface was examined using AFM.

## III. RESULTS AND DISCUSSIONS

Fig. 1 shows the anticipated movie' XRD styles. All the films were polycrystalline. At 37.32°, 43.28°, and 62.70°, respectively, peaks were visible that were attributed to the (111), (200), and (220) planes. These features a typical JCPDS card No (04-0835) [19, 20]. The direction of (200) showed a clear peak, well supported by other researchers [21].

Scherer's equation is applied to make a prediction of the grain size, denoted by "D." [22-24]:

$$D = \frac{0.9\lambda}{\beta cos\theta} \qquad (1)$$

Where λ is X-rays intensity, □ is (FWHM).

According to Table 1, *D* for NiO and NiO: 3% Sb films are 17.81 nm and 28.49 nm, respectively. As antimony doping levels rise, grain size increases due to grain growth [25, 26].

The dislocation density ($\delta$) was calculated by Eq. 2 [27-29]:

$$\delta = \frac{1}{D^2} \qquad (2)$$

The strain (ε) is gained via the relation [30-32]:

$$\varepsilon = \frac{\beta cos\theta}{4} \qquad (3)$$

The structural parameters $S_{para}$ are display in Table 1. Increasing the amount of doping with antimony results in a reduction of the value of strain [33, 34]. Figure (2) lists $S_{para}$ against Antimony content.

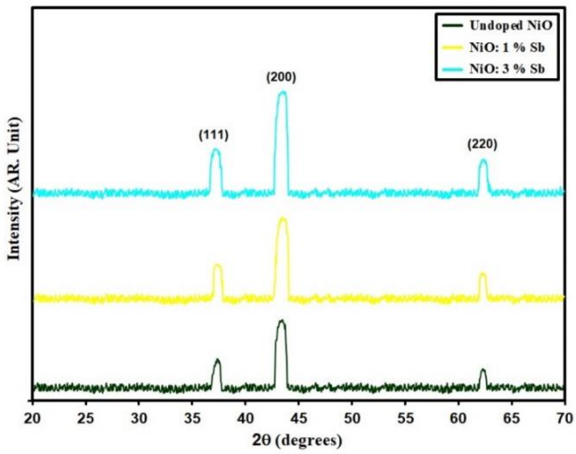


Fig. 1 XRD styles of grown films.

The surface abrasiveness and root-mean-square of the planned films are examined using AFM images. Crystallites with regular sizes and dense packing are visible in Fig. 3's AFM scans. For the necessary films, the typical Pav particle diameter was 87.5, 49.7, and 41.6 nm. undated NiO and NiO: Sb films exhibit roughness on the surface (Ra) and root mean square roughness (Rms) in the range of (10.71-5.26) nm (8.76-3.32), respectively, according to AFM. Ra has decreased as a result of increased grain output [35–37]. In Figure 3, Ra and Rms are shown. The Ra and Rms with antimony content are displayed in Table 2.

TABLE 1. Grown-up flicks D, Eg, and Spara.

| **Sample** | **2 q (º)** | **(hkl) Plane** | **β (º)** | **$E_g$ (eV)** | **Grain area (nm)** | **disconnection density ($\delta$) (× $10^{14}$) (lines/m$^2$)** | **shear(ε) (× $10^{-4}$)** |
|---|---|---|---|---|---|---|---|
| Unreval NiO | 43.28 | 200 | 0.48 | 3.63 | 17.81 | 31.52 | 19.46 |
| NiO: 1% Sb | 43.25 | 200 | 0.42 | 3.56 | 20.35 | 24.14 | 17.03 |
| NiO: 3% Sb | 43.21 | 200 | 0.36 | 3.52 | 2849 | 12.16 | 12.16 |

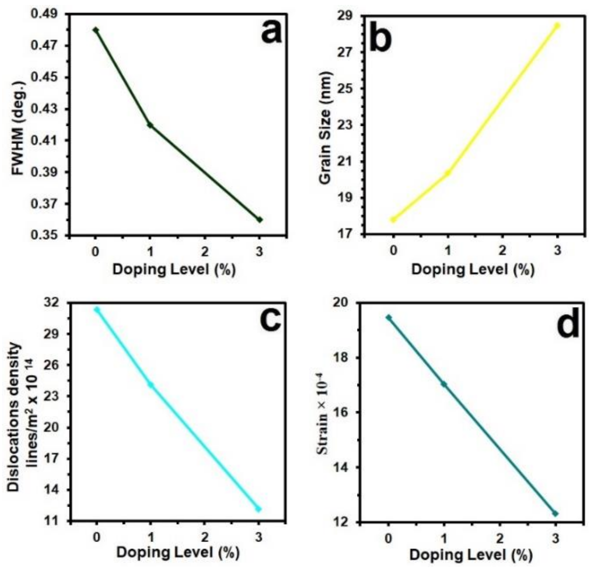


Fig. 2 $S_{para}$ of the delibrate feature.

TABLE 1. AFM parameters of grown films.

| **Samples** | **Pav nm** | **$R_a$ (nm)** | **Rms (nm)** |
|---|---|---|---|
| Undoped NiO | 87.5 | 10.71 | 8.76 |
| NiO: 1% Sb | 49.7 | 9.47 | 6.32 |

| | | | |
|---|---|---|---|
| NiO: 3% Sb | 41.6 | 5.26 | 3.32 |

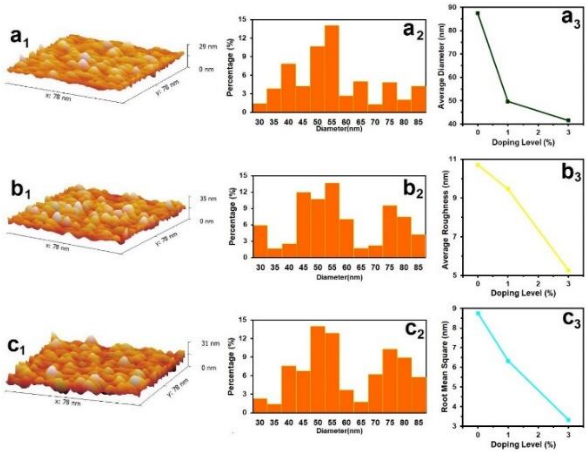


Fig. 3 AFM results of grown films

In Fig. 4, optical characteristics of the intended films doped with antimony at 1% and 3% are depicted. With antimony doping, the transmittance (T) spectra showed a decrease. This suggests that the addition of Antimony to the films affects their optical properties [38,39].

The absorption coefficient (α) is gained by Eq.4 [40-42]:

$$\alpha = \frac{\ln(1/T)}{d} \qquad (4)$$

Where $d$ is film thickness. Figure 5 illustrates a shift in α. In the visible range of the wavelength, all films show a high absorption coefficient with a value of $10^4$ ($cm^{-1}$), indicating a direct transition [43, 44]. As antimony content rises, the absorption coefficient rises as well.

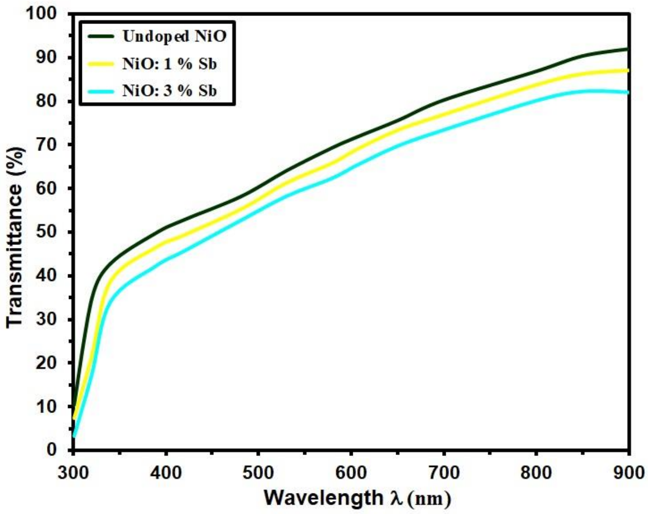


Fig. 4 T of the grown films.

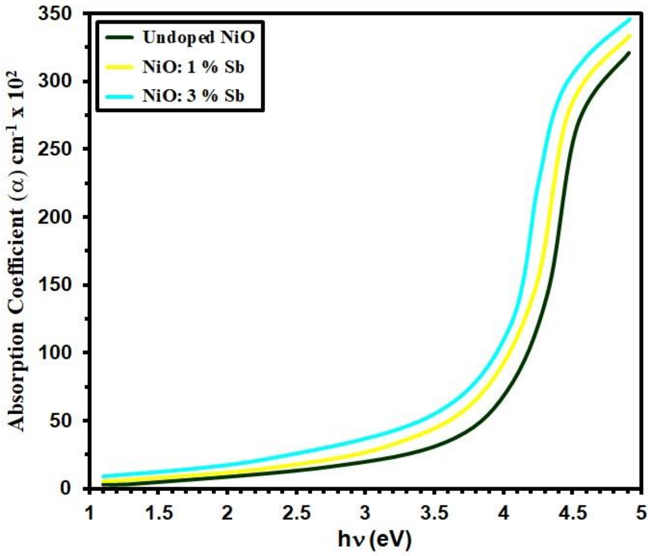


Fig. 5 α Vs hν of the prepared films.

Tauc's relation can be used to evaluate the bandgap energy $E_g$ [46-48]:

$$(\alpha h\nu) = A\left(h\nu - E_g\right)^{\frac{1}{2}} \qquad (5)$$

where A is a constant, Fig. 5. displays that When antimony concentration increased, the energy gap for all produced films reduced. The energy difference ranged from 3.63 to 3.52 eV [49, 50].

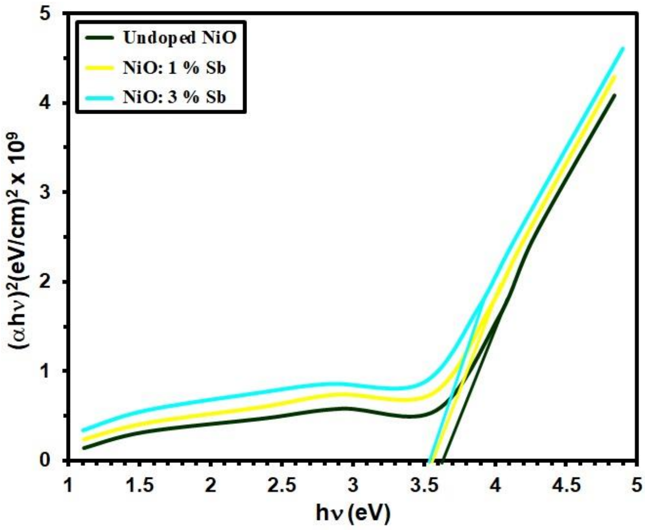


Fig. 6 $E_g$ of the intended films.

The calculated value of (α) was gained to estimate the values of the extinction coefficient (k) utilizing the relation [51-53]:

$$k = \frac{\alpha\lambda}{4\pi} \qquad (6)$$

Where λ is the wavelength. For all the films under investigation, Fig. 7 depicts the extinction coefficient's dependency on wavelength. It is evident that when the doping Antimony proportion increases, the extinction coefficient decreases [54, 55]. an approach to determining the value of the refractive index (n) is to make use of the reflectance (R) spectrum [56-58]:

$$R = \left(\frac{n-1}{n+1}\right)^2 \qquad (7)$$

The value of n was determined by applying the formula below [59-61]:

$$n = \frac{1+\sqrt{R}}{1-\sqrt{R}} \qquad (8)$$

All films displayed comparable behavior in the refractive index spectra, as seen in Fig. 8. It is evident that n decreases as the amount of doped antimony increases [62, 63], The density and surface roughness are to blame for the refractive index's small decrease [64, 65].

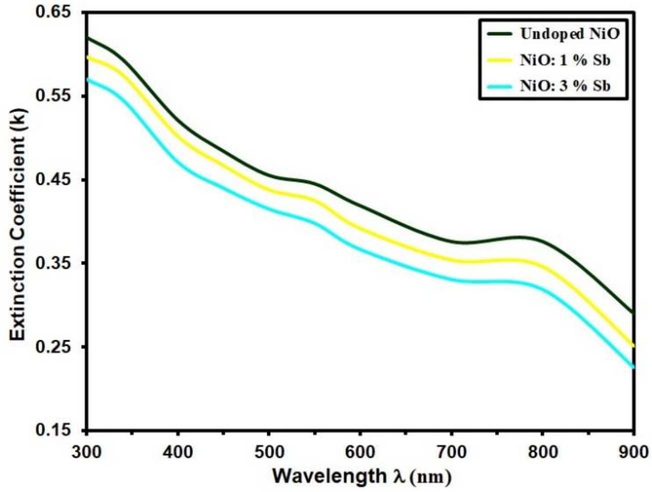


Fig. 7 k of the grown films.

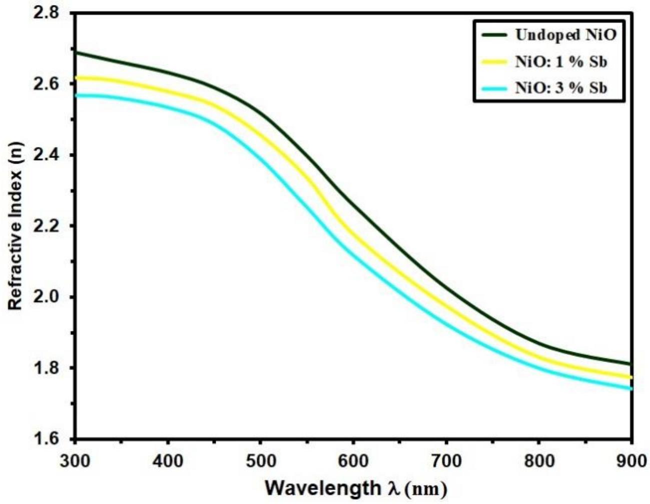


Fig. 8 n for grown films.

## IV. CONCLUSION

The nanostructured matter undated NiO and NiO: Sb thin films were made using a low-cost plasma pyrolysis method. NiO and undeleted NiO: Sb. XRD patterns reveal that the samples are polycrystalline with a preferred (200) orientation. The generated films with XRD measurements showed grains between 17.81 and 28.49 nm, misfit densities between 31.52 and 12.16, and strains between 19.46 and 12.16. The median diameter for the doped samples was discovered to be (87.5), (49.7), and (41.6) nm, respectively. The transmittance decreases as arsenic concentration increases. The optical band gap value reduces from 3.63 eV to 3.52 eV when antimony concentration increases, although n and k increase.

ACKNOWLEDGMENT

This initiative has received financial assistance from Alnukhba University College and Mustansiriyah University (www.mustansiryah.edu.iq).

References


[1] H. Kawazoe, M. Yasukawa, H. Hyodo, M. Kurita, H. Yanagi, H. Hosono, "P-type electrical conduction in transparent thin films of $CuAlO_2$", Nature 389 (1997): 939–942.

[2] G. Thomas, "invisible circuit, Nature 389 (1997): 907–908.

[3] Xinman Chen, Lingzhizhao, and Qiaoliniu. "Electrical and optical properties of ptype Li,Cu-codoped NiO thin films", Electron Mater. 41 (2012): 3382–3386.

[4] R. Sharmaa, A. D. Acharyaa, S. B. Shrivastavaa, T. Shripathi, V. Ganesanb, "Preparation and characterization of transparent NiO thin films deposited by spray pyrolysis technique", Optik 125 (2014): 6751–6756.

[5] C. Parka, J. Kima, K. Leea, S. K. Oha, H. J. Kanga, N. S. Park, "Electronic, optical and electrical properties of nickel oxide thin films grown by RF magnetron sputtering", Appl. Sci. Converg. Technol. 24 (2015): 72–76.

[6] D. S. Kim, H. C. Lee, "Nickel vacancy behavior in the electrical conductance of nonstoichiometric nickel oxide film", J. Appl. Phys. 112 (2012): 1–5.

[7] H. Moulki, C. Faure, M. Mihelcic, A. Surca Vuk, F. Svegl, B. Orel, G. Campet, A.V. Chadwick, D. Gianolio, A. Rougier, M. Alfredsson, "Electrochromic performances of nonstoichiometric NiO thin films", Thin Solid Films. 553 (2014): 63–66.

[8] S. Y. Park, H. R. Kim, Y.J. Kang, D. H. Kim, J. W. Kang, "Organic solar cells employing magnetron sputtered p-type nickel oxide thin film as the anode buffer layer", Sol. Energy Mater. Sol. Cells 94 (2010): 2332–2336.

[9] J. Jung, D.L. Kim, S. H. Oh, H. J. Kim, "Stability enhancement of organic solar cells with solution-processed nickel oxide thin films as hole transport layers", Sol. Energy Mater. Sol. Cells 102 (2012): 103–108.

[10] I. Hotovy, L. Spiess, M. Predanocy, V. Rehacek, J. Racko, "Sputtered nanocrystalline NiO thin films for very low ethanol detection", Vacuum 107 (2014): 129–131.

[11] J. Bandara, C. M. Divarathne, S. D. Nanayakkara, "Fabrication of n-p junction electrodes made of n-type SnO2 and p-type NiO for control of charge recombination in dye sensitized solar cells", Sol. Energy Mater. Sol. Cells 81 (2004): 429–437.

[12] N. S. Das, B. Saha, R. hapa, G. C. Das , K. K. hattopadhyay, "Band gap widening of nanocrystalline nickel oxide thin films via phosphorus doping, Band gap widening of nanocrystalline nickel oxide thin films via phosphorus doping", physics E 42 (2010): 1377-1382.

[13] Y. Zhou, D. H.Gu, Y. Y. Geng, F. X. Gan, "structural and optical properties of NiOx thin films deposited by reactive dc-magnetron sputtering", Mater Sci. Eng. B 135 (2006): 125-128.

[14] Y. R. Park, K. J. Kim, "Sol–gel preparation and optical characterization of NiO and Ni1−xZnxO thin films", J. Cryst. Growth 258 (2003): 380-384.

[15] M.O. Dawood, S. S.Chiad, A. J. Ghazai, N. F. Habubi, O. M. Abdulmunem, "Effect of Li doping on structure and optical properties of NiO nano thin-films by SPT", AIP Conference Proceedings 2213 (2020): 020102.

[16] H.T. Salloom, E. H. Hadi, N. F. Habubi, S. S. Chiad, M. Jadan, J. S. Addasi, "Characterization of silver content upon properties of nanostructured nickel oxide thin films", Digest Journal of Nanomaterials and Biostructures 15(4) (220): 1189-1195.

[17] K. G. Mohammed, I. R. Agool, F. S. Abdulameer, N. F. Habubi, S. S. Chiad, "Investigation of Nanostructured NiO and Au Doped NiO Thin Films by SPT", IOP Conference Series: Earth and Environmental Sciencethis link is disabled 790(1) (2021): 012080.

[18] B. A. Reguig, A. Khelil, L. Cattin, M. Morsli, J.C. Bernede, "Properties of NiO thin films deposited by intermittent spray pyrolysis process". Appl. Surf. Sci. 253 (2007) 4330-4334.

[19] M. A. Hameed, O. A. Ali, and S. S. M. Al-Awadi, "Optical properties of Ag-doped nickel oxide thin films prepared by pulsed-laser deposition technique", Optik 206 (2020): 164352.

[20] P. Salunkhe, M. A. A.V, and D. Kekuda, "Structural, spectroscopic and electrical properties of dc magnetron sputtered NiO thin films and an insight into different defect states", Appl. Phys. A 127 (5) (2021): 390.

[21] W. C Yeh, M. Matsumura, "Chemical vapor deposition of nickel oxide films from bis-π-cyclopentadienyl-nickel", Jpn. J. Appl. Phys. 36 (1997): 6884-6887.

[22] E. S. Hassan, A. K. Elttayef, S. H. Mostafa, M. H. Salim, S. S. Chiad, “Silver oxides nanoparticle in gas sensors applications”, Journal of Materials Science: Materials in Electronics 30(17) (2019):15943-15951,.

[23] E. H. Hadi, M. A. Abbsa, A. A. Khadayeir, Z. M. Abood, N. F. Habubi, S. S. Chiad, “Effects of Mn doping on the characterization of nanostructured TiO2thin films deposited via chemical spray pyrolysis method”, Journal of Physics: Conference Series 1664 (1), (2020).

[24] R. S. Ali, M. K. Mohammed, A. A. Khadayeir, Z. M. Abood, Habubi, N. F., S.S. Chiad, “Structural and Optical Characterization of Sprayed nanostructured Indium Doped $Fe_2O_3$Thin Films”, Journal of Physics: Conference Series 1664(1) (2020): 012016.

[25] B. Subramanian, M. M. Ibrahim, K. R. Murali, Vidhya VS, Sanjeeviraja C, Jayachandran M. “Structural, optoelectronic and electrochemical properties of nickel oxide films”, J. Mater Sci. Mater Electron. 20 (2009): 953-957.

[26] M. H. Raza et al., “Tuning the NiO Thin Film Morphology on Carbon Nanotubes by Atomic Layer Deposition for Enzyme-Free Glucose Sensing”, ChemElectroChem 6 (2) (2019): 383–392.

[27] A. J. Ghazai, O. M. Abdulmunem, K. Y. Qader, S. S. Chiad, N. F. Habubi, “Investigation of some physical properties of Mn doped ZnS nano thin films”, AIP Conference Proceedings 2213 (1) (2020): 020101.

[28] E. S. Hassan, K. Y. Qader, E. H. Hadi, S. S. Chiad, N. F. Habubi, K. H. Abass, “Sensitivity of nanostructured mn-doped cobalt oxide films for gas sensor application”, Nano Biomedicine and Engineering, 12(3) (2020): 205-213.

[29] M. S. Othman, K. A. Mishjil, H. G. Rashid, S. S. Chiad, N. F. Habubi, I. A. Al-Baidhany, “Comparison of the structure, electronic, and optical behaviors of tin-doped CdO alloys and thin films”, Journal of Materials Science: Materials in Electronics 31(11) (2020): 9037-9043.

[30] N. N. Jandow, M. S. Othman, N. F. Habubi, S. S. Chiad, K. A. Mishjil, I. A. Al-Baidhany, “Theoretical and experimental investigation of structural and optical properties of lithium doped cadmium oxide thin films”, Materials Research Express 6(11) (2020).

[31] A. A. Khadayeir, E. S. Hassan, T. H. Mubarak, S. S. Chiad, N. F. Habubi, M. O. Dawood, I. A. Al-Baidhany,“The effect of substrate temperature on the physical properties of copper oxide films”, Journal of Physics: Conference Series 1294 (2) (2019): 022009.

[32] E. H. Hadi, D. A. Sabur, S. S. Chiad, N.F. Habubi, K. H. Abass, “Physical properties of nanostructured li-doped $zro_2$ thin films”, Journal of Green Engineering 10 (10) (2020): 8390-8400.

[33] V. Gowthami, P. Perumal, R. Sivakumar, C.Sanjeeviraja, “Structural and optical studies on nickel oxide thin film prepared by nebulizer technique”, Physica B, 452 (2014): 1-6.

[34] R. A. Ismail, S. Ghafori, G. A. Kadhim, "Preparation and characterization of nanostructurednickel oxide thin films by spray pyrolysis",ppl.Nanosci. 3 (2013): 509-514.

[35] A. Sharma, R. K. Srivastava, S. Kumar, S. K. Singh, “Investigation of Antimony Doped Nickel Oxide Thin films on Physical Properties by Spray Pyrolysis Technique”, Materials Today Proceedings 2 (4-5) (2015): 2664-2670.

[36] A. Singh, V. Singh, R. Shrivastav, “Investigation of Antimony Doped Nickel Oxide Thin Films on Physical Properties by Spray Pyrolysis Technique”, Journal of Materials Science: Materials in Electronics, 30 (22) (2019): 19357-19366.

[37] M. Moradi, M. Ramezani, “Investigation of the effect of antimony doping on the physical properties of nickel oxide thin films deposited by spray pyrolysis” Applied Physics A, 123 (3) (2017): 1-8.

[38] K. O. Ukoba, A. C. Eloka-Eboka F. L. Inambao, “Review of nanostructured NiO thin film deposition using the spray pyrolysis technique”, Renewable and Sustainable Energy Reviews 82 (2018): 2900–2915.

[39] B. R. Cruz-Ortiz, M. A. Garcia-Lobato, E. R. Larios-Duran, E. M. Muzquiz-Ramos, and J. C. Ballesteros-Pacheco, “Potentiostatic electrodeposition of nanostructured NiO thin films for their application as electrocatalyst”, Journal of Electroanalytical Chemistry 772 (2016): 38–45.

[40] M. D. Sakhil, Z. M. Shaban, K. S. Sharba, N. F. Habub, K. H. Abass, S. S. Chiad, A. S. Alkelaby, “Influence mgo dopant on structural and optical properties of nanostructured cuo thin films, NeuroQuantology 18 (5) (2020) 56-61.

[41] S. S. Chiad, H. A. Noor, O. M. Abdulmunem, N. F. Habubi, M. Jadan, J.S. Addasi, “Optical and structural performance of nanostructured Te thin films by (CSP) with various thicknesses”, Journal of Ovonic Research 16 (1)(2020): 35-40.

[42] H. A. Hussin, R. S. Al-Hasnawy, R. I. Jasim, N. F. Habubi, S. S. Chiad, “Optical and structural properties of nanostructured CuO thin films doped by Mn”, Journal of Green Engineering 10(9) (2020): 7018-7028.

[43] N. F. Al.Shammary: "Optical characteristics of NiO thin film on glass formed by Chemical spray pyrolysis", JOURNAL OF KUFA – PHYSICS 2 (1), (2010).

[44] A. R. Balu , V. S. Nagarethinam a, N. Arunkumar b, M. Suganya, "Nanocrystalline NiO thin films prepared by A low cost simplified spray technique using perfume atomizer", Journal of Electron Devices 13 (2012): 920-930.

[45] B. Sasi, K. G. Gopchandran, P. K. Manoj, et al. "Preparation of transparent and semiconducting NiO films", Vacuum. 68,( 2003):149–154.

[46] S. S. Chiad, A. S. Alkelaby, K. S. Sharba, Optical Conduct of Nanostructure Co3O4 rich Highly Doping $Co_3O_4$: Zn alloys" Journal of Global Pharma Technology 11(7) (2020): 662-665.

[47] N. Y. Ahmed, B. A. Bader, M. Y. Slewa, N. F. Habubi, S. S. Chiad, "Effect of boron on structural, optical characterization of nanostructured $fe_2o_3$ thin films", NeuroQuantology 18 (6) (2020): 55-60,.

[48] A. A., Jasim R. I., S. H. Jumaah, N. F. Habubi, S. S. Chiad, "Influence of Khadayeir Substrate Temperature on Physical Properties of Nanostructured ZnS Thin Films", Journal of Physics: Conference Series1664 (1) (2020).

[49] S. C Chen, T. Y. Kuo, Y. C. Lin, C. L. Chang, "Preparation and properties of p-type transparent conductive NiO films", Adv Mater Res, 123 (2020):181–184.

[50] J.-H. Yu, S.-H. Nam, Y. E. Gil, J.-H. Boo, "The effect of ammonia concentration on the microstructure and electrochemical properties of NiO nanoflakes array prepared by chemical bath deposition", Applied Surface Science 532 (2020): 147441.

[51] R. S. Ali, N. A. H. Al Aaraji, E. H. Hadi, K. H Abass, N. F. Habubi, S. S Chiad, "Effect of Lithium on Structural and Optical Properties of anostructured CuS Thin", Journal of Nanostructuresthis link is disabled 10(4) (2020): 810–816.

[52] A. S. Al Rawas, M. Y. Slewa, B. A. Bader, N. F. Habubi, S.S. Chiad, "Physical characterization of nickel doped nanostructured $TiO_2$ thin films", Journal of Green Engineering10 (9) (2020): 7141-7153.

[53] E. S. Hassan, T. H. Mubarak, S. S. Chiad, N. F. Habubi, A. A. Khadayeir, M.O. Dawood, I.A. Al-Baidhany, "Physical Properties of indium doped Cadmium sulfide thin films prepared by (SPT) ", Journal of Physics: Conference Series 1294 (2) (2019).

[54] I. Hotovy, V. Rehacek, P. Siciliano, S. Capone, L. Spiess, "Sensing characteristics of NiO thin films as $NO_2$ gas sensor", Thin Solid Films 418 (2002): 9–15.

[55] H. Lee, Y.-T. Huang, M. W. Horn, S.-P. Feng, "Engineered optical and electrical performance of rf– sputtered undoped nickel oxide thin films for inverted perovskite solar cells", Sci Rep 8 (1) (2018):5590.

[56] S. S. Chiad, N. F. Habubi, W. H. Abass, M. H. Abdul-Allah, "Effect of thickness on the optical and dispersion parameters of $Cd_{0.4}Se_{0.6}$ thin films", Journal of Optoelectronics and Advanced Materials, 18(9-10) (2016): 822-826.

[57] A. A. Khadayeir, E. S. Hassan, S. S. Chiad, N. F. Habubi, K. H. Abass, M. H. Rahid, T. H. Mubarak, M. O. Dawod I. A. Al-Baidhany, "Structural and Optical Properties of Boron Doped Cadmium Oxide", Journal of Physics: Conference Series 1234 (1) (20119): 012014

[58] H. T. Salloom, R. I. Jasim, N. F. Habubi, S. S. Chiad, M. Jadan, J. S. Addasi, "Gas sensor using gold doped copper oxide nanostructured thin films as modified cladding fiber", Chinese Physics Bthis link is disabled 30(6) (2021):068505.

[59] K. Y. Qader, R. A. Ghazi, A. M. Jabbar, K. H. Abass, S. S. Chiad, "Reduce of energy gap of CuO nano structure film by Ag doping", Journal of Green Engineering 10 (10) (2020): 7387-7398.

[60] B. A. Bader, S. K. Muhammad, A. M. Jabbar, K. H. Abass, S.Salman Chiad and N. F. Habubi, "Synthesis and Characterization of Indium-doped CdO Nanostructured Thin Films: a Study on Optical", orphological, and Structural Properties, J. Nanostruct 10(4) (2020): 744-750.

[61] E. S. Hassan, A. K. Elttayef, S. H. Mostafa, M. H. Salim, S. S. Chiad, "Silver oxides nanoparticle in gas sensors applications", Journal of Materials Science: Materials in Electronics 30 (17) (2019): 15943-15951.

[62] I. Manouchehri, D. Mehrparvar, R. Moradiana, K. Gholami, T., "Investigation of structural and optical properties of copper doped NiO Osati thin films deposited by RF magnetron reactive sputtering", Optik 127 (2016) :8124–8129.

[63] R. Paulose, R. Mohan, and V. Parihar, "Nanostructured nickel oxide and its electrochemical behaviour—A brief review", Nano-Structures & Nano-Objects 11(2017): 102–111.

[64] K. R.C, Bukovec P., “Sol–gel prepared NiO thin films for electrochromic applications”, Acta Chim Slov 53 (2006):136–147.

[65] I. M. Chan, F.C. Hong, "Improved performance of the single-layer and double-layer organic light emitting diodes by nickel oxide coated indium tin oxide anode”, Thin Solid Films 450 (2004):304–311.